Journal of Solid Mechanics Vol. 15, No. 1 (2023) pp. 50-65
DOI: 10.22034/jsm.2021.1938490.1715

Research Paper

Vibration Behavior of Thick Sandwich Composite Beam with Flexible Core Resting on Incompressible Fluid Foundation

M. Khosravi [1], S. Jafari Mehrabadi [1,*], K. Malekzadeh Fard [2]

[1]*Department of Mechanical Engineering, Arak Branch, Islamic Azad University, Arak, Iran*
[2]*Department of Structural Engineering and Simulations, Malek Ashtar University of Technology, Tehran, Iran*

Received 20 September 2022; accepted 12 December 2022

ABSTRACT

In this research, free flexural vibration of a thick sandwich composite beam that is made up of two composite face sheets and a flexible foam-made core based on a fluid is investigated. Governing equations for the sandwich beam were extracted using a higher-order theory. The face sheets were modeled using the first-order shear deformation theory (FSDT). In the analysis of the multilayer sandwich composite beam, the layers and the core in the middle were assumed to be well attached to one another, and continuous strain functions at the layer interfaces were assumed. Moreover, displacements were assumed to be small, so that the analyses could be performed in linear elastic region with simply supported boundary condition for the beam. Equations of motion of the beam were extracted using energy equations and Hamilton's principle. Continuing with the research, effects of changing different parameters were evaluated; these included core thickness to total thickness ratio, beam length to total thickness ration, face sheet material, fluid density, and fluid height. The results showed that the presence of the liquid tend to lower the natural frequency of the structure. Our investigations further indicated that the natural frequency follows an increasing trend with decreasing the fluid density.

Keywords: Free vibration; Thick composite beam; Flexible core; Fluid Foundation; Higher-order theory.

1 INTRODUCTION

DURING the recent decades, sandwich structures and multilayer orthotropic composites have found widespread applications in various industries, including the aerospace industries and marine, civil, and mechanical structures. This has been thanks to relatively high strength-to-weight coupled with excellent flexural stiffness of such advanced material. Accordingly, a number of research works have been performed to estimate natural

[*]Corresponding author. Tel.: +98 086 33412563.
E-mail address: s-jafari@iau-arak.ac.ir (S. Jafari Mehrabadi)

frequency of sandwich structures. Frostig and Thomson presented an investigation into free vibration of sandwich panels with flexible cores using the higher-order theory. In this work, they analyzed the face sheets and the core using the classical and 3D elasticity theories, respectively, ignoring in-plane strains. Their calculations were based on two models. The first model took the shear strain in the core and displacements of the top and bottom face sheets as unknowns. This model was based on the assumption that the core transmits the inertial loads into the face sheets rather than withstanding them, *i.e.*, distribution of acceleration along the thickness of the core was in the form of a static displacement field under extended loading. The second model assumed a polynomial distribution for the displacement field in the core, where the unknowns included the coefficients of the polynomial and face sheet displacements. The main advantage of this methodology was the direct incorporation of dynamic loads into the core equation, eliminating the need for considering the core interactions with the top and bottom face sheets [1]. Amirani *et al.* studied free vibration of a sandwich beam with a functionally graded (FG) core. In this research, the element-free Galerkin (EFG) method was used to formulate 2D elasticity problems, with the so-called penalty method used to handle the core- face sheet relationships in the sandwich beam [2]. Banerjee *et al.* analyzed free vibration of the three-layer sandwich beam at different beam thicknesses. They used the Timoshenko's beam theory to simulate the displacement field for each layer and derive the equations of motion (EoMs). Subsequently, they considered an exact dynamic stiffness model into which harmonic variables were incorporated, with the Wittrick-Williams algorithm further employed to enhance the accuracy of the results. Comparing their findings to experimental data, they reported very good agreement [3]. Damanpack and Khalili focused on higher-order free vibration of sandwich beams with flexible core using dynamic stiffness method. Using the Hamilton's principle, they derived the EoM for a single element and then expanded it to numerous elements to build a system of equations with seven differential equations. Finally, they calculated natural frequencies and mode shapes for symmetric sandwich beam and discussed their results [4]. Khdeir and Aldraihem undertook to analyze free vibration of sandwich beams with flexible core using the so-called zigzag theory. Following this approach, they managed to obtain natural frequency and mode shapes of the system using the state space and compared their results to experimental data as well as analytic and numerical results. Their solution method was comparable to approximation methods like Rayleigh-Ritz method, finite-element technique, and other numerical procedures [5]. Salami *et al.* adopted the higher-order theory to analyze sandwich beams with soft core and fiber-reinforced carbon nanotube (CNT) face sheets. Performing micromechanical modeling, they considered uniform or FG distribution of fibers along the face sheet thickness, assuming that the face sheet follows first-order shear deformation theory (FSDT) [6]. Stoykov and Margenov investigated nonlinear vibration of 3D layered composite beams. For this purpose, they used the Timoshenko's beam under flexural loading for beam analysis. Their results showed that the natural frequency of the beam was determined by the placement angle of the layers [7]. Robinson and Palmer performed modal analysis of a rectangular plate floated on top of an incompressible fluid at lower frequencies under the effect of small-amplitude surface waves. In this work, they derived the governing vibration equations for the plate-fluid system [8]. Hosseini-Hashemi *et al.* investigated free vibration of simply supported Mindlin plates in contact with a fluid using a semi-analytic method. First, they developed an implicit analytic solution by separation of variables. They then applied the Ritz method onto the plate domain to extract final governing equations [9]. In another piece of research, Hosseini-Hashemi *et al.* studied free vibration of a horizontal rectangular plate submerged in floated on top of the free surface of a fluid for six different conlurations, namely two parallel edges with simple supports and the other two edges subjected to different boundary conditions. In this work, equations governing the relatively thick rectangular plate was obtained based on those for a Mindlin plate, with the velocity potential function and Bernoulli's equation used to evaluate the pressure exerted to the free surface of the plate [10]. Rezvani *et al.* studied the effect of added mass on the natural frequencies of the structure and fluid. They began by performing a frequency analysis and then verified their results against experimental data and numerical findings [11]. Esmailzadeh *et al.* obtained free vibration of the structures that contained or were submerged into a fluid. They used potential function for assessing the hydrodynamic pressure applied to the structure and concluded that the fluid depth imposes a great impact on the structure-fluid interactions [12]. Li *et al.* investigated free vibration of the beams made from FG material into variable thicknesses and submerged into a fluid. They adopted the Hamilton's principle, Timoshenko's beam model, and boundary conditions to derive EoMs of the beam before estimating the natural frequency of the beam using the DQ method [13].

In this research, free flexural vibration of a thick sandwich composite beam that is made up of two composite face sheets and a flexible foam-made core based on an incompatible fluid is investigated. Innovation and the difference between this article and other similar works are express in two cases:

1. Differences between different fluid densities on the natural frequency of the structure.
2. The effect of fluid height as a substrate on the natural frequency of the structure.

Also, the effect of physical parameters such as the effects of changing parameters such as core thickness to total beam thickness, beam length to total thickness on the vibration response of the system, has been investigated.

2 CONSIDERED GEOMETRY

In the present research, a sandwich beam with two composite face sheets and one flexible core was studied (Fig.1). Thicknesses of the top and bottom face sheets and the core are herein denoted by h_t, h_b, and h_c, respectively. The considered coordinate system is depicted in Fig. 1, with the indices *t* and *b* referring to the top and bottom face sheets, respectively. The following assumptions are made in this work:

1. For analyzing the multilayer sandwich composite beam, the layers and the middle core are attached to one another, with the strain function being continuous at the interface of different layers.
2. Layer placement in the sandwich composite beam is symmetric and balanced.
3. Simply supported boundary conditions for the considered beam.

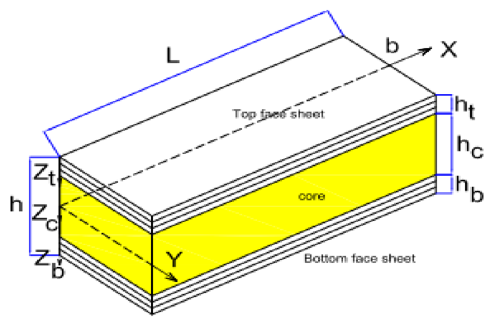

Fig.1
Geometry and dimensions of the sandwich beam [14].

3 GOVERNING EQUATIONS OF MOTION

3.1 Face sheet displacement fields

In the present work, the face sheets were modeled by FSDT. Accordingly, displacement fields of different face sheets in the Cartesian coordinate system takes the form of Eq. (1) [15]:

$$u_j(x,z_j,t)=u_0^j(x,t)+\phi_x^j(x,t)\,z_j \qquad (j=t,b) \qquad (1)$$
$$w_j(x,z_j,t)=w_0^j(x,t)$$

where $u_0^j(x,t)$ is the displacement component in the *x* direction in the mid-plane, $w_0^j(x,t)$ is the displacement component in the *z* direction in the mid-plane, and $\phi_0^j(x,t)$ denotes the cross-sectional rotation around the *x*-axis in the top and bottom face sheet.

3.2 Core displacement field

According to Frostig's second model (Frostig and Thomson, 2004), the core displacement field was modeled by third-order and quadratic functions of z_c for its in-plane and out-of-plane components, respectively.

$$u_c(x,z_c,t)=u_0^c(x,t)+u_1^c(x,t)z_c+u_2^c(x,t)z_c^2+u_3^c(x,t)z_c^3$$
$$w_c(x,z_c,t)=w_0^c(x,t)+w_1^c(x,t)z_c+w_2^c(x,t)z_c^2 \qquad (2)$$

In which $u_0^c(x,t)$, $u_1^c(x,t)$, $u_2^c(x,t)$ and $u_3^c(x,t)$ denote in-plane displacement components in *x* direction and $w_0^c(x,t)$, $w_1^c(x,t)$ and $w_2^c(x,t)$ refer to out-of-plane displacement components in *z* direction at the middle plane of the core.

3.3 Displacement strain relationships for core and face sheets

Considering Eqs. (1) and (2) and the linear strain assumption, the following equations describe the relationships between the strains and displacements [1]:

$$\varepsilon_{xx}=\frac{\partial u\,(x,z)}{\partial x}\ ,\quad \varepsilon_{zz}=\frac{\partial w\,(x,z)}{\partial z}\ ,\quad \varepsilon_{xz}=\frac{1}{2}[\frac{\partial u\,(x,z)}{\partial z}+\frac{\partial w\,(x,z)}{\partial x}] \tag{3}$$

Substituting Eqs. (1) and (2) into Eq. (3) gives:

$$\begin{aligned} &\varepsilon_{xx}^{j}=u_{0,x}^{j}+z_j\phi_{x,x} \\ &\gamma_{xz}^{j}=\phi_x+w_{0,x}^{j} \end{aligned}\qquad (j=t,b) \tag{4}$$

$$\begin{aligned} &\varepsilon_{xx}^{c}=u_{0,x}^{c}+u_{1,x}^{c}z_c+u_{2,x}^{c}z_c^{2}+u_{3,x}^{c}z_c^{3} \\ &\varepsilon_{zz}^{c}=w_1^{c}+2w_2^{c}z_c \\ &\gamma_{xz}^{c}=(u_1^{c}+w_{0,x}^{c})+(2u_2^{c}+w_{1,x}^{c})z_c+(3u_3^{c}+w_{2,x}^{c})z_c^{2} \end{aligned} \tag{5}$$

3.4 Compatibility condition

One of the assumptions made in this analysis was no separation between the core and face sheets. That is, we herein assumed complete continuity between the core and top and the bottom face sheets during the loading and deformation stages occurred to the sandwich beam. The face sheets and the middle core are assumed to be well attached to another, with the strain function being continuous at the core- face sheet interface. Accordingly, compatibility condition at the interface between the core and faces sheets, which somewhat couples the core equations to those of the top and bottom face sheets, takes the following form:

$$\begin{aligned} &u_c(z=z_{cj})=u_0^{j}+\frac{1}{2}(-1)^{k}h_j\phi_{xj} \\ &w_c(z=z_{cj})=w_0^{j} \end{aligned} \tag{6}$$

when $j = t$, then $k = 0$ and $z_{ct}=-\frac{h_c}{2}$. Moreover, if $j = b$, then $k = 1$ and $z_{cb}=-\frac{h_c}{2}$. Now, substituting Eqs. (1) and (2) into Eq. (6), compatibility condition at the core- face sheet interface is derived as follows:

$$\begin{aligned} &u_0+u_1\frac{h_c}{2}+u_2\frac{h_c^2}{2}+u_3\frac{h_c^3}{2}=u_0^b-\phi_x^b\frac{h_b}{2} \\ &w_0+w_1\frac{h_c}{2}+w_2\frac{h_c^2}{2}=w_0^b \\ &u_0-u_1\frac{h_c}{2}+u_2\frac{h_c^2}{2}-u_3\frac{h_c^3}{2}=u_0^t+\phi_x^t\frac{h_b}{2} \\ &w_0-w_1\frac{h_c}{2}+w_2\frac{h_c^2}{2}=w_0^t \end{aligned} \tag{7}$$

One can reduce the number of unknowns by writing some coefficient as functions of other coefficients, as expressed in the following:

$$\begin{aligned} u_2 &= (2(u_0^b + u_0^t) - h_b\phi_x^b + h_t\phi_x^t - 4u_0)/h_c^2 \\ u_3 &= (4(u_0^b - u_0^t) - 2(h_b\phi_x^b + h_t\phi_x^t) - 4h_c u_1)/h_c^3 \\ w_2 &= (2(w_0^b + w_0^t) - 2w_0)/h_c^2 \\ w_1 &= 2(w_0^b - w_0^t)/h_c \end{aligned} \tag{8}$$

According to the above equation, the number of unknowns for the core decreased to 3. Energy method and Hamilton's principle were utilized to extract the governing equations and boundary conditions in this research [16]:

$$\int_{t_1}^{t_2} (\delta U - \delta T)\, dt = 0 \tag{9}$$

where T and U are kinetic and potential energies, respectively, and t refers to the period delineated by the times t_1 and t_2.

3.5 Total strain energy variation

$$\delta U = \int_{v_t} (\sigma_{xx}^t \delta\varepsilon_{xx}^t + \tau_{xz}^t \delta\gamma_{xz}^t)dV_t + \int_{v_b} (\sigma_{xx}^b \delta\varepsilon_{xx}^b + \tau_{xz}^b \delta\gamma_{xz}^b)dV_b + \int_{v_t} (\sigma_{xx}^c \delta\varepsilon_{xx}^c + \sigma_{zz}^c \delta\varepsilon_{zz}^c + \tau_{xz}^c \delta\gamma_{xz}^c)dV_c \tag{10}$$

3.6 Total kinetic energy variation

$$\delta T = \int_{vt} (\rho_t(\dot{u}_t\, \delta\dot{u}_t + \dot{w}_t\, \delta\dot{w}_t)dv_t + \int_{vb} (\rho_b(\dot{u}_b\, \delta\dot{u}_b + \dot{w}_b\, \delta\dot{w}_b)dv_b + \int_{vc} (\rho_c(\dot{u}_c\, \delta\dot{u}_c + \dot{w}_c\, \delta\dot{w}_c)dv_c \tag{11}$$

In general, stress resultants on the face sheets are defined as stress components, as follows:

$$N_{xx}^j = \int_{-\frac{b_j}{2}}^{\frac{b_j}{2}} \int_{-\frac{h_j}{2}}^{\frac{h_j}{2}} \sigma_{xx}^j\, dz_j\, dy_j \quad , \quad M_{xx}^j = \int_{-\frac{b_j}{2}}^{\frac{b_j}{2}} \int_{-\frac{h_j}{2}}^{\frac{h_j}{2}} \sigma_{xx}^j z_j\, dz_j\, dy_j \quad , \quad Q_{xz}^j = \int_{-\frac{b_j}{2}}^{\frac{b_j}{2}} \int_{-\frac{h_j}{2}}^{\frac{h_j}{2}} \tau_{xz}^j\, dz_j\, dy_j \qquad j = t,b \tag{12}$$

Given that the considered structure is a sandwich beam with multilayer composite face sheets, stress resultants of the face sheets are defined as follows:

$$\begin{aligned} \{N^j\} &= [A_{11}^j]\{u_{0j,x}\} + [B_{11}^j]\{\phi_{x,x}^j\} \\ \{M^j\} &= [B_{11}^j]\{u_{0j,x}\} + [D_{11}^j]\{\phi_{x,x}^j\} \\ \{Q_{xz}^j\} &= k\,[A_{55}^j]\{\phi_x^i + w_{,x}^i\} \qquad j = t,b \end{aligned} \tag{13}$$

In Eq. (13), k is the shear correction factor, which is herein set to 5/6 [17]. The components A_{mn}^j, B_{mn}^j and D_{mn}^j (*m, n* =1,5 and *j= t, b*) are the components of the tensile and flexural stiffness matrices [15].

$$\begin{aligned} A_{mn} &= \sum_{k=1}^{N} (\bar{Q}_{mn})_k (z_k - z_{k-1}) \\ B_{mn} &= \frac{1}{2}\sum_{k=1}^{N} (\bar{Q}_{mn})_k (z_k^2 - z_{k-1}^2) \qquad \text{m=n=1,5} \\ D_{mn} &= \frac{1}{3}\sum_{k=1}^{N} (\bar{Q}_{mn})_k (z_k^3 - z_{k-1}^3) \end{aligned} \tag{14}$$

In general, when the layers are at an angle of θ with respect to the original coordinate, stress vs. reduced strain relationship for the k^{th} layer can be expressed as follows:

$$\begin{Bmatrix}\sigma_{xx}\\ \sigma_{yy}\\ \sigma_{zz}\\ \sigma_{xy}\\ \sigma_{xz}\\ \sigma_{yz}\end{Bmatrix}^K = \begin{bmatrix}\bar{Q}_{11} & \bar{Q}_{12} & \bar{Q}_{13} & \bar{Q}_{14} & 0 & 0\\ \bar{Q}_{12} & \bar{Q}_{22} & \bar{Q}_{23} & \bar{Q}_{24} & 0 & 0\\ \bar{Q}_{13} & \bar{Q}_{23} & \bar{Q}_{33} & \bar{Q}_{34} & 0 & 0\\ \bar{Q}_{14} & \bar{Q}_{24} & \bar{Q}_{34} & \bar{Q}_{44} & 0 & 0\\ 0 & 0 & 0 & 0 & \bar{Q}_{55} & \bar{Q}_{56}\\ 0 & 0 & 0 & 0 & \bar{Q}_{56} & \bar{Q}_{66}\end{bmatrix}^K \begin{Bmatrix}\varepsilon_{xx}\\ \varepsilon_{yy}\\ \varepsilon_{zz}\\ \gamma_{xy}\\ \gamma_{xz}\\ \gamma_{yz}\end{Bmatrix}^K \tag{15}$$

The following equation defines stress resultants in the core as a function of stress components:

$$\begin{Bmatrix}N_{xx}^c\\ M_{xx}^c\\ P_{xx}^c\\ H_{xx}^c\end{Bmatrix} = \int_{-\frac{b_c}{2}}^{\frac{b_c}{2}}\int_{-\frac{h_c}{2}}^{\frac{h_c}{2}} \begin{Bmatrix}1\\ z_c\\ z_c^2\\ z_c^3\end{Bmatrix}\sigma_{xx}^c\, dz_c\, dy_c \quad , \begin{Bmatrix}N_{zz}^c\\ M_{zz}^c\end{Bmatrix} = \int_{-\frac{b_c}{2}}^{\frac{b_c}{2}}\int_{-\frac{h_c}{2}}^{\frac{h_c}{2}} \begin{Bmatrix}1\\ z_c\end{Bmatrix}\sigma_{zz}^c\, dz_c\, dy_c$$

$$\begin{Bmatrix}Q_{xz}^c\\ L_{xz}^c\\ R_{xz}^c\end{Bmatrix} = \int_{-\frac{b_c}{2}}^{\frac{b_c}{2}}\int_{-\frac{h_c}{2}}^{\frac{h_c}{2}} \begin{Bmatrix}1\\ z_c\\ z_c^2\end{Bmatrix}\tau_{xz}^c\, dz_c\, dy_c \tag{16}$$

Moments of inertia for the face sheets and the core are defined as follows:

$$\begin{Bmatrix}I_{0J}\\ I_{1yJ}\\ I_{2yJ}\end{Bmatrix} = \int_{-\frac{b_j}{2}}^{\frac{b_j}{2}}\int_{-\frac{h_j}{2}}^{\frac{h_j}{2}} \rho_{0j}\begin{Bmatrix}1\\ z_j\\ z_j^2\end{Bmatrix} dz_j\, dy_j \qquad j = t,b$$

$$(I_{0c},\ I_{1yc}, I_{2yc},\ I_{3yc},\ I_{5yc},\ I_{6yc}) = \int_{-\frac{b_c}{2}}^{\frac{b_c}{2}}\int_{-\frac{h_c}{2}}^{\frac{h_c}{2}} \rho_{0c}(1, z_c, z_c^2, z_c^3, z_c^4, z_c^5, z_c^6)\, dz_c\, dy_c \tag{17}$$

4 GOVERNING EQUATIONS FOR THE FLUID

In order to model the dynamic behavior of a fluid (Fig.2) with a density of ρ_f, we begin by analyzing the solid-fluid interactions at their interface using a mathematical model.

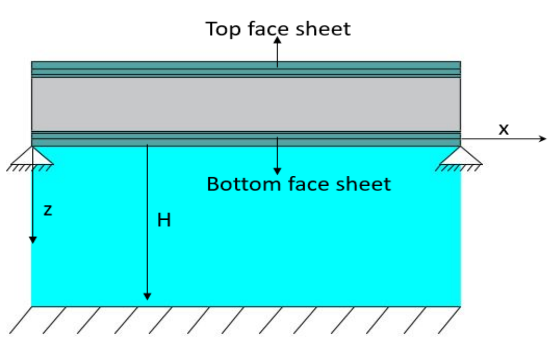

Fig.2
Beam and fluid configuration.

This mathematical model is based on the following assumptions [9,18]:

- Fluid flow is in potential mode.
- Fluid is ideal, *i.e.* incompressible, non-rotational, and inviscid.
- Stationary fluid flow velocity is zero.

Based on the first assumption (potential nature of the fluid flow), one can calculate the velocity potential using Eq. (18):

$$\nabla^2\psi = \frac{\partial^2\psi}{\partial x^2} + \frac{\partial^2\psi}{\partial z^2} = 0 \tag{18}$$

where $\psi = \psi(x, z, t)$ denotes velocity potential function of the fluid. Now, in order to apply boundary conditions for the fluid, one may notice that Eq. (19) shall be satisfied in the beam-fluid contact area for particular velocities in *z* direction (applying Bernoulli's equation and ignoring non-rotational terms)[10]:

$$\frac{\partial\psi}{\partial z}\Big|_{z=\frac{h_b}{2}} = \frac{\partial w}{\partial t} \tag{19}$$

Other boundary conditions for the considered structure in terms of the position of supports (x = 0, L) and fluid depth (z = H) are as explained in Eq. (20):

$$\frac{\partial\psi}{\partial z}\Big|_{z=H} = 0 \quad , \quad \frac{\partial\psi}{\partial x}\Big|_{x=0,L} = 0 \tag{20}$$

Applying the separation of variables technique onto the velocity potential function then gives:

$$\psi(x, z, t) = F(z)\, G(x, t) \tag{21}$$

$$\xrightarrow{(21)\to(19)} G(x, t) = \frac{\partial w}{\partial t} \frac{1}{\left.\frac{dF}{dz}\right|_{z=-\frac{h_b}{2}}} \tag{22}$$

$$\xrightarrow{(22)\to(21)} \psi(x, z, t) = \frac{F(z)}{\left.\frac{dF}{dz}\right|_{z=-\frac{h_b}{2}}} \frac{\partial w}{\partial t} \tag{23}$$

$$\Rightarrow \frac{d^2F(z)}{dz^2} - \mu_f^2\, F(z) = 0 \tag{24}$$

$$\Rightarrow F(z) = B_1 e^{\mu_f z} + B_2 e^{-\mu_f z} \tag{25}$$

$$\xrightarrow{(23)\ and\ (25)} \psi(x, z, t) = \frac{B_1 e^{\mu_f z} + B_2 e^{-\mu_f z}}{\left.\frac{dF}{dz}\right|_{z=-\frac{h_b}{2}}} \frac{\partial w}{\partial t} \tag{26}$$

Therefore, kinetic energy of the fluid can be obtained from Eq. (27):

$$T_f = \frac{1}{2}\rho_f \int_v \Delta\psi \,.\, \Delta\psi \; dv \tag{27}$$

Obtaining kinetic energy of the fluid and adding it to that of the structure and substituting the stress resultants of the core and face sheets into the Hamilton's principle, Equations of motion can be extracted as follows.

5 EQUATIONS OF MOTION

$$
\begin{aligned}
&\delta u_{0t}:\ (-N^{t}_{xx,x}-\frac{2}{h_c^2}P^{c}_{xx,x}+\frac{4}{h_c^3}H^{c}_{xx,x}+\frac{4}{h_c^2}L^{c}_{xz}-\frac{12}{h_c^3}R^{c}_{xz})+I_0\ddot{u}_{0t}+I_{1y}\ddot{\phi}_{xt}\\
&-(-\frac{2}{h_c^2}I_{2y}+\frac{4}{h_c^3}I_{3y}+\frac{8}{h_c^4}I_{4y}-\frac{16}{h_c^5}I_{5y})\ddot{u}_{0c}-(-\frac{2}{h_c^2}I_{3y}+\frac{4}{h_c^3}I_{4y}+\frac{8}{h_c^4}I_{5y}-\frac{16}{h_c^5}I_{6y})\ddot{u}_{1c}\\
&-(-\frac{4}{h_c^4}I_{4y}+\frac{8}{h_c^5}I_{5y}-\frac{8}{h_c^5}I_{5y}+\frac{16}{h_c^6}I_{6y})\ddot{u}_{0t}-(-\frac{4}{h_c^4}I_{4y}+\frac{8}{h_c^5}I_{5y}-\frac{8}{h_c^5}I_{5y}+\frac{16}{h_c^6}I_{6y})\ddot{u}_{0b}\\
&-(-\frac{h_t}{h_c}I_{4y}+\frac{2h_t}{h_c^3}I_{5y}-\frac{2h_t}{h_c^5}I_{5y}-\frac{8h_t}{h_c^6}I_{6y})\ddot{\phi}_t-(-\frac{h_b}{h_c}I_{4y}-\frac{2h_b}{h_c^3}I_{5y}+\frac{2h_t}{h_c^5}I_{5y}-\frac{8h_b}{h_c^6}I_{6y})\ddot{\phi}_b=0
\end{aligned}
\tag{28}
$$

$$
\begin{aligned}
&\delta\phi_t:-(-M^{t}_{xx,x}+Q^{t}_{xz}-\frac{h_t}{h_c^2}P^{c}_{xx,x}+\frac{2h_t}{h_c^3}H^{c}_{xx,x}+\frac{2h_t}{h_c^2}L^{c}_{xz}-\frac{6h_t}{h_c^3}R^{c}_{xz})+I_{1y}\ddot{u}_{0t}+I_{2y}\ddot{\phi}_{xt}\\
&-(-\frac{h_t}{2}I_{2y}+\frac{2h_t}{h_c^3}I_{3y}+\frac{2h_t}{h_c^2}I_{4y}-\frac{8h_t}{h_c^5}I_{5y})\ddot{u}_{0c}-(-\frac{h_t}{2}I_{3y}+\frac{2h_t}{h_c^3}I_{4y}+\frac{2h_t}{h_c^2}I_{5y}-\frac{8h_t}{h_c^5}I_{6y})\ddot{u}_{1c}\\
&-(-\frac{h_t}{h_c^2}I_{4y}+\frac{4h_t}{h_c^5}I_{5y}+\frac{2h_t}{h_c^3}I_{5y}-\frac{8h_t}{h_c^6}I_{6y})\ddot{u}_{0t}-(-\frac{h_t}{h_c^2}I_{4y}+\frac{4h_t}{h_c^5}I_{5y}-\frac{2h_t}{h_c^3}I_{5y}+\frac{8h_t}{h_c^6}I_{6y})\ddot{u}_{0b}\\
&-(-\frac{h_t^2}{4}I_{4y}+\frac{h_t^2}{h_c^3}I_{5y}+\frac{h_t^2}{h_c^3}I_{5y}-\frac{4h_t^2}{h_c^6}I_{6y})\ddot{\phi}_{xt}-(\frac{h_th_b}{4}I_{4y}+\frac{h_th_b}{h_c^3}I_{5y}+\frac{h_th_b}{h_c^3}I_{5y}-\frac{8h_th_b}{h_c^6}I_{6y})\ddot{\phi}_{xb}=0
\end{aligned}
\tag{29}
$$

$$
\begin{aligned}
&\delta w_{0t}:\ (-Q^{t}_{xz,x}-\frac{1}{h_c}N^{c}_{zz}+\frac{4}{h_c^2}M^{c}_{zz}+\frac{1}{h_c}L^{c}_{xz,x}-\frac{2}{h_c^2}R^{c}_{xz,x})+I_0\ddot{w}_{0t}\\
&-(\frac{1}{h_c}I_{1y}-\frac{2}{h_c^2}I_{2y}-\frac{4}{h_c^3}I_{3y}+\frac{8}{h_c^4}I_{4y})\ddot{w}_{0c}-(\frac{1}{h_c^2}I_{2y}+\frac{2}{h_c^3}I_{3y}+\frac{2}{h_c^3}I_{3y}-\frac{4}{h_c^4}I_{4y})\ddot{w}_{0t}\\
&-(\frac{1}{h_c^2}I_{2y}-\frac{2}{h_c^3}I_{3y}+\frac{2}{h_c^3}I_{3y}+\frac{4}{h_c^4}I_{4y})\ddot{w}_{0b}=0
\end{aligned}
\tag{30}
$$

$$
\begin{aligned}
&\delta u_{0b}:(-N^{b}_{xx,x}-\frac{2}{h_c^2}P^{c}_{xx,x}-\frac{4}{h_c^3}H^{c}_{xx,x}+\frac{4}{h_c^2}L^{c}_{xz}+\frac{12}{h_c^3}R^{c}_{xz})+I_0\ddot{u}_{0b}+I_{1y}\ddot{\phi}_{xb}\\
&-(-\frac{2}{h_c^2}I_{2y}-\frac{4}{h_c^3}I_{3y}+\frac{8}{h_c^4}I_{4y}+\frac{16}{h_c^5}I_{5y})\ddot{u}_{0c}-(-\frac{2}{h_c^2}I_{3y}-\frac{4}{h_c^3}I_{4y}+\frac{8}{h_c^4}I_{5y}+\frac{16}{h_c^5}I_{6y})\ddot{u}_{1c}\\
&-(-\frac{4}{h_c^4}I_{4y}+\frac{8}{h_c^5}I_{5y}+\frac{8}{h_c^5}I_{5y}+\frac{16}{h_c^6}I_{6y})\ddot{u}_{0t}-(-\frac{4}{h_c^4}I_{4y}+\frac{8}{h_c^5}I_{5y}-\frac{8}{h_c^5}I_{5y}-\frac{16}{h_c^6}I_{6y})\ddot{u}_{0b}\\
&-(-\frac{h_b}{h_c^2}I_{4y}-\frac{2h_t}{h_c^3}I_{5y}+\frac{2h_t}{h_c^5}I_{5y}-\frac{8h_t}{h_c^6}I_{6y})\ddot{\phi}_t-(-\frac{h_b}{h_c^2}I_{4y}+\frac{2h_b}{h_c^3}I_{5y}+\frac{2h_b}{h_c^5}I_{5y}+\frac{8h_b}{h_c^6}I_{6y})\ddot{\phi}_b=0
\end{aligned}
\tag{31}
$$

$$\begin{aligned}&\delta\phi_b:(-M^b_{xx,x}+Q^b_{xz}+\frac{h_b}{h_c^2}P^c_{xx,x}+\frac{2h_b}{h_c^3}H^c_{xx,x}-\frac{2h_b}{h_c^2}L^c_{xz}-\frac{6h_b}{h_c^3}R^c_{xz})+I_{1y}\ddot{u}_{0b}+I_{2y}\ddot{\phi}_{xb}\\&-(\frac{h_b}{2}I_{2y}+\frac{2h_b}{h_c^3}I_{3y}-\frac{2h_b}{h_c^2}I_{4y}-\frac{8h_b}{h_c^5}I_{5y})\ddot{u}_{0c}-(\frac{h_b}{2}I_{3y}+\frac{2h_b}{h_c^3}I_{4y}-\frac{2h_b}{h_c^2}I_{5y}-\frac{8h_b}{h_c^5}I_{6y})\ddot{u}_{1c}\\&-(\frac{h_b}{h_c^2}I_{4y}+\frac{4h_b}{h_c^5}I_{5y}-\frac{2h_b}{h_c^3}I_{5y}-\frac{8h_b}{h_c^6}I_{6y})\ddot{u}_{0t}-(\frac{h_b}{h_c^2}I_{4y}+\frac{4h_b}{h_c^5}I_{5y}+\frac{2h_b}{h_c^3}I_{5y}+\frac{8h_b}{h_c^6}I_{6y})\ddot{u}_{0b}\\&-(\frac{h_t h_b}{4}I_{4y}+\frac{h_t h_b}{h_c^3}I_{5y}+\frac{h_t h_b}{h_c^3}I_{5y}-\frac{4h_t h_b}{h_c^6}I_{6y})\ddot{\phi}_{xt}-(-\frac{h_b^2}{4}I_{4y}-\frac{h_b^2}{h_c^3}I_{5y}-\frac{h_b^2}{h_c^3}I_{5y}-\frac{4h_b^2}{h_c^6}I_{6y})\ddot{\phi}_{xb}=0\end{aligned}\tag{32}$$

$$\begin{aligned}&\delta w_{0b}:(-Q^b_{xz,x}+\frac{1}{h_c}N^c_{zz}+\frac{4}{h_c^2}M^c_{zz}-\frac{1}{h_c}L^c_{xz,x}-\frac{2}{h_c^2}R^c_{xz,x})+I_0\ddot{w}_{0b}\\&-(-\frac{1}{h_c}I_{1y}-\frac{2}{h_c^2}I_{2y}+\frac{4}{h_c^3}I_{3y}+\frac{8}{h_c^4}I_{4y})\ddot{w}_{0c}-(-\frac{1}{h_c^2}I_{2y}+\frac{2}{h_c^3}I_{3y}-\frac{2}{h_c^3}I_{3y}-\frac{4}{h_c^4}I_{4y})\ddot{w}_{0t}\\&-(-\frac{1}{h_c^2}I_{2y}-\frac{2}{h_c^3}I_{3y}-\frac{2}{h_c^3}I_{3y}-\frac{4}{h_c^4}I_{4y})\ddot{w}_{0b}-b.\rho_f.\psi.\ddot{w}_{0b}=0\end{aligned}\tag{33}$$

$$\begin{aligned}&\delta u_{0c}:(-N^c_{xx,x}+\frac{4}{h_c^2}P^c_{xx,x}-\frac{8}{h_c^2}L^c_{xx,x})-(-I_0+\frac{8}{h_c^2}I_{2y}-\frac{16}{h_c^4}I_{4y})\ddot{u}_{0c}\\&-(-I_{1y}+\frac{4}{h_c^2}I_{3y}+\frac{4}{h_c^2}I_{3y}-\frac{16}{h_c^4}I_{6y})\ddot{u}_{1c}-(-\frac{2}{h_c^2}I_{2y}+\frac{8}{h_c^4}I_{4y}+\frac{4}{h_c^3}I_{3y}-\frac{16}{h_c^5}I_{6y})\ddot{u}_{0t}\\&-(-\frac{2}{h_c^2}I_{2y}+\frac{8}{h_c^4}I_{4y}-\frac{4}{h_c^3}I_{3y}+\frac{16}{h_c^5}I_{6y})\ddot{u}_{0b}-(-\frac{h_t}{2}I_{2y}+\frac{4h_t}{2h_c^2}I_{4y}+\frac{2h_t}{h_c^3}I_{3y}-\frac{8h_t}{h_c^5}I_{5y})\ddot{\phi}_t\\&-(\frac{h_b}{2}I_{2y}-\frac{4h_b}{2h_c^2}I_{4y}+\frac{2h_b}{h_c^3}I_{3y}-\frac{8h_b}{h_c^5}I_{5y})\ddot{\phi}_b=0\end{aligned}\tag{34}$$

$$\begin{aligned}&\delta u_{1c}:(-M^c_{xx,x}+\frac{4}{h_c^2}H^c_{xx,x}+Q^c_{xz}-\frac{12}{h_c^2}R^c_{xx,x})\\&-(-I_{1y}+\frac{8}{h_c^2}I_{3y}-\frac{16}{h_c^4}I_{5y})\ddot{u}_{0c}-(-I_{2y}+\frac{4}{h_c^2}I_{4y}+\frac{4}{h_c^2}I_{4y}-\frac{16}{h_c^4}I_{5y})\ddot{u}_{1c}\\&-(-\frac{2}{h_c^2}I_{3y}+\frac{8}{h_c^4}I_{5y}+\frac{4}{h_c^3}I_{4y}-\frac{16}{h_c^5}I_{6y})\ddot{u}_{0t}-(-\frac{2}{h_c^2}I_{3y}+\frac{8}{h_c^4}I_{5y}-\frac{4}{h_c^3}I_{4y}+\frac{16}{h_c^5}I_{6y})\ddot{u}_{0b}\\&-(-\frac{h_t}{2}I_{3y}+\frac{4h_t}{2h_c^2}I_{5y}+\frac{2h_t}{h_c^3}I_{4y}-\frac{8h_t}{h_c^5}I_{6y})\ddot{\phi}_t-(\frac{h_b}{2}I_{3y}-\frac{4h_b}{2h_c^2}I_{5y}+\frac{2h_b}{h_c^3}I_{4y}-\frac{8h_b}{h_c^5}I_{6y})\ddot{\phi}_b=0\end{aligned}\tag{35}$$

$$\begin{aligned}&\delta w_{0c}:-(-\frac{8}{h_c^2}M^c_{zz}-Q^c_{xz}+\frac{4}{h_c^2}R^c_{xz,x})-(-I_0+\frac{8}{h_c^2}I_{2y}-\frac{16}{h_c^4}I_{4y})\ddot{w}_{0c}\\&-(\frac{1}{h_c}I_{1y}-\frac{4}{h_c^3}I_{3y}-\frac{2}{h_c^2}I_{2y}+\frac{8}{h_c^4}I_{4y})\ddot{w}_{0t}-(-\frac{1}{h_c}I_{1y}+\frac{4}{h_c^3}I_{3y}-\frac{2}{h_c^2}I_{2y}+\frac{8}{h_c^4}I_{4y})\ddot{w}_{0t}=0\end{aligned}\tag{36}$$

5.1 Solving the equations of motion

A common approach to solving governing equations of the problems concerning free vibration of simply supported sandwich composite beams is to use a Fourier transform that satisfies all boundary conditions. For a simply supported beam, one may use the Fourier transform as expressed in the following equations.

$$\begin{bmatrix} u_0^i(x,y,t) \\ w_0^i(x,y,t) \\ \phi_x^i(x,y,t) \\ u_k(x,y,t) \\ w_l(x,y,t) \end{bmatrix} = \sum_{m=1}^{M} \begin{bmatrix} C_{u_0^i}^m(t)\cos(\alpha_m x) \\ C_{w_0^i}^m(t)\sin(\alpha_m x) \\ C_{\phi_x^i}^m(t)\cos(\alpha_m x) \\ C_{uk}^m(t)\cos(\alpha_m x) \\ C_{wl}^m(t)\sin(\alpha_m x) \end{bmatrix} \quad (37)$$

where $i= t, b$ refers to the top and bottom face sheets, respectively. Moreover, K (K = 0, 1, 2, 3) and l (l = 0, 1, 2), $\alpha_m = \frac{mn}{a}$, where m is the half wave numbers in x directions and a is the length of the beam. Where $C_{u_0^i}^m, C_{w_0^i}^m, C_{\phi_x^i}^m, C_{uk}^m, C_{wk}^m$ are the time dependent coefficients to be determined.

The abovementioned functions are applicable to symmetric and balanced composite face sheets, in which case we have:

$$A_{16}^i = A_{26}^i = B_{16}^i = B_{26}^i = D_{16}^i = D_{26}^i = 0 \quad (38)$$

In which $j=t, b$. Using Eqs. (9) and (37), one can write a system of differential equations for the beam based on planar and transverse displacement and rotation functions for the face sheets and the middle core, as follows:

$$[M]\{\ddot{\chi}\}+[K]\{\chi\}=0 \quad (39)$$

5.2 Validation and discussion on numerical results

In this section, in order to validate the proposed model and demonstrate the performance and accuracy of the methodology developed for solving Eq. (39), the results are compared to the reported data in published works at credible journals.

Case 1: Analyzing the vibration of a sandwich beam with foam-made core and isotropic face sheet. In this case, a sandwich beam with simply supported boundary conditions and a geometry and core and face sheets properties defined in Fig. 3 was considered [19].

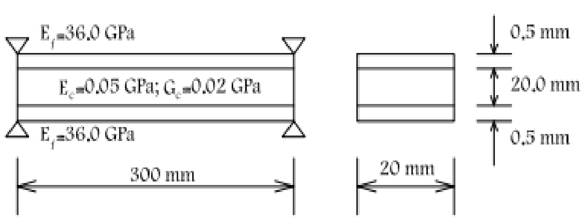

Fig.3
Geometrical model of sandwich beam [19].

The results obtained using the methodology proposed in this article regarding the free vibration are reported in Table 1, where those are further compared to previously published results that were obtained through analytical procedures[19-21] and finite-element method [19].

Table 1 indicates that the natural frequencies obtained from the proposed methodology were in good agreement with previously reported results. Indeed, the observed differences could be attributed to different choices for representing the core displacement field. Moreover, Refs [19-21] used 5 governing equations, while the proposed theory in this work described the problem using 9 governing equations. This implies more complete mathematical modeling of the problem, thereby lowering the system error down to an acceptable level.

Table 1
Natural frequencies of the sandwich beam in Hz.

Mode number	Frostig and Baruch[20]	Yang and Qiao [19]	ABAQUS [19]	Rahmani et al. [21]	Present work	Percentage difference Frostig and Baruch [20]	Percentage difference Yang and Qiao [19]	Percentage difference Rahmani et. al. [21]
	325.98	325.98		326.39	334.30699	2.55	2.55	2.43
	4287	4767.31		4767.31	4526.3691	5.58	5.05	5.05
m=1	6518.11	6769.24	349.86	6777.76	6683.8948	2.54	1.26	1.38
	7304.78	7304.79		7311.82	7308.9806	0.06	0.06	0.04
	825.3	824.96		826.62	834.17395	1.08	1.12	0.91
	7304.8	7304.85		7311.87	7332.3235	0.38	0.38	0.28
m=2	8574	9534.62	777.42	9534.63	8859.426	3.33	7.08	7.08
	10278.7	10674.7		10680.08	10684.796	3.95	0.09	0.04
	1310.38	1308.9		1311.84	1319.4966	0.70	0.81	0.58
	7305.01	7305.05		7312.08	7356.5329	0.71	0.70	0.61
m=3	12861	14301.9	1657.33	14301.94	12616.131	1.90	11.79	11.79
	14520.4	15080		15083.8	15119.41	4.13	0.26	0.24

Case 2: Analyzing the vibration of a sandwich composite beam with foam-made core and orthotropic face sheet. According to Fig. 4, a sandwich beam with a foam-made core and symmetric three-layer composite face sheets was considered. For the sake of modeling, the top and bottom face sheets were layered under the [0, 90, 0] scheme [19, 22, 23].

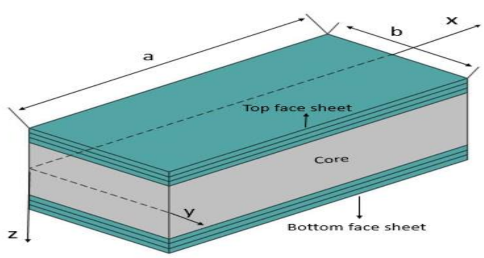

Fig.4
Sandwich beam with foam-made core and composite face sheets.

Face sheet properties:

$$E1 = 172.7GPa \quad , E2 = 7.2GPa \ , \upsilon = .3 \, , \ G12 = 3.76 \quad GPa, \quad G23 = G12 \, , \rho_{faces} = 1566 \ \frac{kg}{m^3}$$

Core properties:

$$E_c = 0.0\,5GPa \quad , \upsilon_c = .3 \, , \ G12 = 0.02 \quad GPa, \quad G23 = G12 \, , \rho_c = 52.06 \ \frac{kg}{m^3}$$

Geometrical configuration of the composite sandwich beam:

$$a = 300mm, \ b = 20mm \, , \ h_c = 20mm \, , \ \mathrm{h}_{\mathrm{plythickness}} = .5mm \quad , N = 3$$

where a and b are the beam length and width, respectively, the subscript c refers to core, $h_{plythickness}$ is the thickness of each layer of the face sheet, and N is the number of the face sheet layers. Table 2 reports the obtained values of natural frequency for the first three modes of the structure. The table further presents the effect of an increase in beam length to total thickness of the sandwich beam on dimensionless frequencies of the sandwich composite beam with foam-made core. The dimensionless frequencies, $\bar{\omega}$, were obtained from the formula $\bar{\omega} = \omega h \sqrt{\frac{\rho_c}{E_c}}$ where ω

denotes natural frequencies, h is the beam thickness, ρ_c is the core density, and E_c is the Young's modulus along the thickness.

Table 2
Effect of increasing beam length to total thickness ratio on dimensionless frequencies of the sandwich beam with foam-made core.

Mode number	$\frac{a}{h}=10$	$\frac{a}{h}=20$	$\frac{a}{h}=30$	$\frac{a}{h}=40$	$\frac{a}{h}=50$
m=1	0.090008627	0.041035597	0.024469113	0.016245337	0.01149585
	1.0464883	1.0453603	0.83128036	0.62657903	0.50235187
	2.0500377	1.2254569	1.0449631	0.94131255	0.85103294
	2.733793	1.4930095	1.1113884	1.0449357	1.0447657
m=2	0.19331649	0.090008277	0.057410135	0.041036641	0.031114579
	1.0532959	1.0464883	1.045587	1.0453603	0.99227693
	2.3426101	2.0500376	1.5815635	1.2254569	1.0449133
	3.0976797	2.5728509	2.0500378	1.7346551	1.259225
m=3	0.31298167	0.14014928	0.090008854	0.065551873	0.050881563
	1.0712979	1.0489456	1.0464883	1.0457653	1.0454688
	2.4699393	2.2619029	1.9001969	1.4930095	1.4456865
	3.9466533	2.7337928	2.5257521	2.1078946	1.7355737

Table 3 considers the effect of increasing core thickness to total thickness ratio on dimensionless frequencies of the sandwich beam with foam-made core.

Table 3
Effect of increasing core thickness to total thickness ratio on dimensionless frequencies of the sandwich beam with foam-made core.

Mode number	$\frac{h_c}{h}=0.1$	$\frac{h_c}{h}=0.2$	$\frac{h_c}{h}=0.3$	$\frac{h_c}{h}=0.4$	$\frac{h_c}{h}=0.5$	$\frac{h_c}{h}=0.7$	$\frac{h_c}{h}=0.9$
m=1	0.0071319	0.0127597	0.0192586	0.0264694	0.0342803	0.0513933	0.0701185
	0.4854326	0.6871888	0.7836778	0.8329824	0.8819776	0.9742383	1.0580442
	0.6737377	0.7398125	0.8827337	1.0707945	1.2491616	1.5629278	1.7907661
	0.7326688	0.7400843	1.0331097	1.2305694	1.4289858	1.8227513	2.2073159
m=2	0.0195215	0.0315291	0.0452039	0.0602154	0.0763566	0.1114380	0.1495546
	0.7327664	0.7408899	0.7841477	0.8337604	0.8831402	0.9764315	1.0616484
	0.9705159	1.3699879	1.7419657	2.0489315	2.2240624	2.2806097	2.2668171
	1.454829	2.0389631	2.4691291	2.5344687	2.6295378	2.6617257	2.7779883
m=3	0.0350444	0.0542733	0.0758398	0.0992619	0.1242517	0.1781315	0.2362345
	0.7331126	0.8409974	0.7855573	0.8359281	0.8862276	0.9818695	1.0701608
	1.0829268	1.4738138	1.8783417	2.2819168	2.3820097	2.4051746	2.3796223
	1.5396613	2.1472495	2.7586434	2.7825661	2.8723705	3.4324064	3.9189691

On Fig. 5, it is clear that any increase in the *L/H* ratio decreases all of the three dimensionless natural frequencies (*i.e.*, the first, second, and third dimensionless natural frequencies). It is then evident that the structure loses some of its stiffness upon increasing this ratio, or say the sandwich beam becomes more flexible, as is demonstrated in Fig. 5.

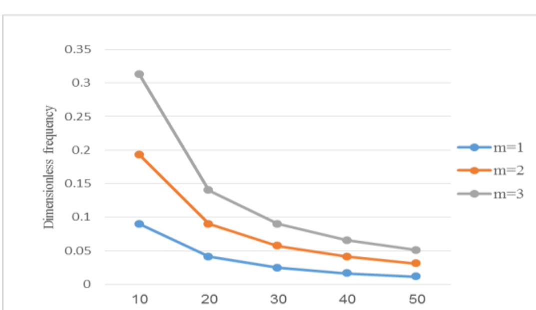

Fig.5
Increasing the beam length to total thickness ratio.

On Fig. 6, it is clearly observed that all of the dimensionless natural frequencies of the beam structure increase with the core thickness to total thickness ratio.

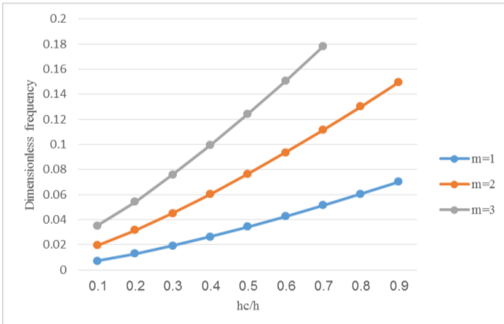

Fig.6
Increasing the core thickness to total thickness ratio.

Case 3: Analyzing the vibration of a sandwich composite beam with foam-made core and orthotropic face sheet on a fluid foundation. In order to analyze vibration of a beam on a fluid foundation, effects of two fluid parameters, namely the fluid height and density, on the vibratory behavior of a beam with the geometrical properties introduced in the Case 2 were investigated. To this end, the first three natural frequencies of the structure were taken into consideration, and the fluid height variations were studied up to the point where these natural frequencies converged to those of the corresponding fluid-free case.

Table 4 presents the properties of the fluids used in this research [24].

Table 4
Fluid properties

Fluid	$\rho\left(kg/m^3\right)$
Gasoline	860
Pure water	1000
Sea water	1025
Glycerin	1261

Table 5
Effects of fluid density and height on the natural frequencies (Hz).

Mode number		$h_f(m)$						
	Fluid	0	0 .001	0 .003	0.005	0 .007	0 .009	0 .01
m=1	Pure water	455.57102	364.1889	441.40165	447.16268	449.02046	449.81623	450.03994
m=2		973.71566	776.67687	943.22202	955.62509	959.62338	961.33589	961.81723
m=3		1540.4661	1224.0047	1491.6887	1511.545	1517.9413	1520.6802	1521.4499
m=1	Sea water	*	362.55502	441.06408	446.95835	448.86025	449.67516	449.90422
m=2		*	773.15178	942.49503	955.18531	959.27865	961.03222	961.52518
m=3		*	1218.335	1490.5243	1510.8413	1517.3899	1520.1946	1520.9829
m=1		*	373.76436	443.30648	448.31203	449.92064	450.60889	450.80223
m=2	Gasoline	*	797.33831	947.32369	958.0988	961.56052	963.04145	963.45752
m=3		*	1257.2425	1498.2574	1515.5026	1521.0394	1523.4075	1524.0728
m=1		*	348.13991	437.91479	445.04318	447.35646	448.34959	448.62897
m=2		*	742.05832	935.71207	951.06269	956.0422	958.17965	958.78094
m=3	Glycerin	*	1168.346	1479.6563	1504.2434	1512.2123	1515.6319	1516.5938

The results reported in Table 5 and depicted in Fig. 7 show that all three natural frequencies (*i.e.*, for the three modes, m = 1, 2, 3) decreased with changing the fluid type to achieve a higher fluid density. The outputs further show that the decrease in the natural frequencies was greater for fluids of higher densities. Therefore, it can be stipulated that glycerin led to the most significant changes in the natural frequency, followed by seawater, pure water, and gasoil, as compared to the case with no fluid foundation.

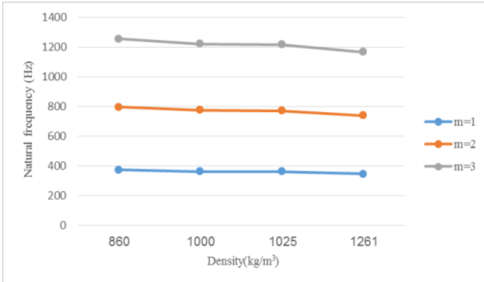

Fig.7
Effect of fluid density on natural frequency.

Figs. 8 through 11 imply that an increase in the fluid height tend to increase the natural frequency. At a given fluid depth, the smallest reduction in frequency was triggered by glycerin, followed by seawater, pure water, and gasoil. Moreover, the higher the fluid density, the higher the required fluid height to have the natural frequencies converged to those of fluid-free structure.

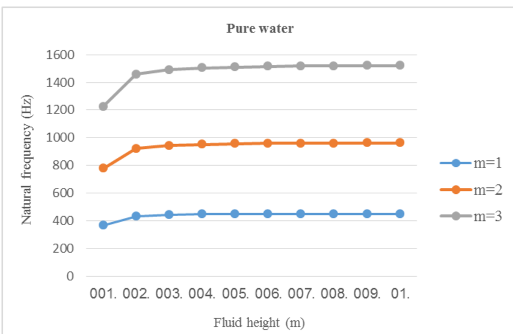

Fig.8
Effect of fluid height on natural frequency.

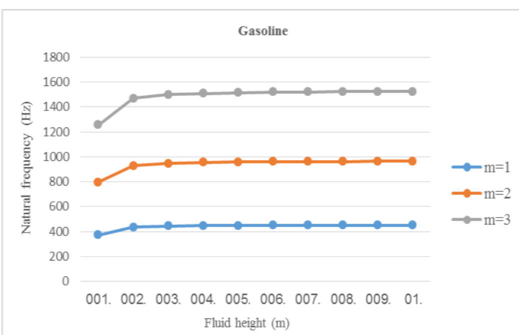

Fig.9
Effect of fluid height on natural frequency.

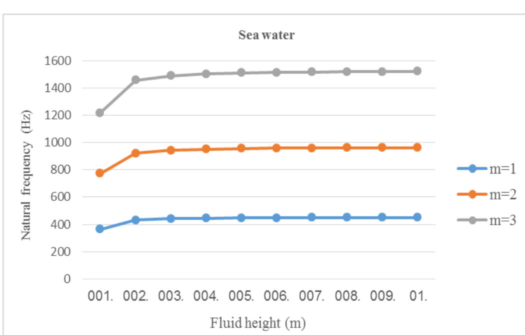

Fig.10
Effect of fluid height on natural frequency.

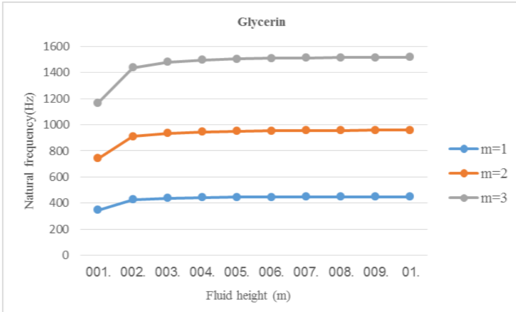

Fig.11
Effect of fluid height on natural frequency.

6 CONCLUSIONS

Natural frequencies of sandwich beams with foam-made cores were investigated under two scenarios:

A. Natural frequency of sandwich beam without the effect of fluid:

In this case, we investigated the effects of beam length to total thickness ratio and core thickness to total thickness ratio, ending up with the following results:

1. The first, second, and third natural frequencies decrease with increasing the beam length to total thickness ratio. It is trivial that an increase in this ratio. according to the relationship $\omega=\sqrt{k/m}$ reduces the effect of structure stiffness or, say, makes the sandwich beam more flexible.
2. The first, second, and third natural frequencies increase linearly with increasing the core thickness to total thickness ratio.

B. Natural frequency of sandwich beam under the effect of fluid:

The presence of a fluid foundation tends to add to the mass matrix of the structure, thereby reducing the natural frequency of the beam, this is due to the increase in the kinetic energy of the beam on the fluid foundation. The natural frequencies were found to increase with the fluid height under the structure. Moreover, lower natural frequencies were observed with denser fluids as the increase in fluid density tends to increase the structure mass at constant stiffness. At a given fluid depth, the smallest reduction in frequency was triggered by glycerin, followed by seawater, pure water, and gasoil.

REFERENCES

[1] Frostig Y.,Thomsen O.T., 2004, High-order free vibration of sandwich panels with a flexible core, *International Journal of Solids and Structures* **41**: 1697-1724.

[2] Amirani M.C., Khalili S.M.R., Nemati N., 2009, Free vibration analysis of sandwich beam with FG core using the element free Galerkin method, *Composite Structures* **90**: 373-379.

[3] Banerjee J.R., 2007, Free vibration of a three-layered sandwich beam using the dynamic stiffness method and experiment, *International Journal of Solids and Structures* **44**: 7543-7563.

[4] Damanpack A.R., Khalili S.M.R., 2012, High-order free vibration analysis of sandwich beams with a flexible core using dynamic stiffness method, *Composite Structures* **94**: 1503-1514.

[5] Khdeir A.A., Aldraihem O.J., 2016, Free vibration of sandwich beams with soft core, *Composite Structures* **154**: 179-189.

[6] Salami S.J., 2016, Extended high order sandwich panel theory for bending analysis of sandwich beams with carbon nanotube reinforced face sheets, *Physica E: Low-Dimensional Systems and Nanostructures* **76**: 187-197.

[7] Stoykov S., Margenov S., 2014, Nonlinear vibrations of 3D laminated composite beams, *Mathematical Problems in Engineering* **1**: 1-14.

[8] Robinson N.J.,Palmer S.C., 1990, A modal analysis of a rectangular plate floating on an incompressible liquid, *Journal of Sound and Vibration* **142**: 453-460.

[9] Hashemi S.H.H., Karimi M., Taher H.R.D., 2010, Vibration analysis of rectangular Mindlin plates on elastic foundations and vertically in contact with stationary fluid by the Ritz method, *Ocean Engineering* **37**: 174-185.

[10] Hosseini-Hashemi S., Karimi M., Rokni H., 2012, Natural frequencies of rectangular Mindlin plates coupled with stationary fluid, *Applied Mathematical Modelling* **36**: 764-778.

[11] Rezvani S.S., 2015, Effects of added mass parameter on fluid-structure natural frequencies by using analytical, numerical and experimental methods, *Amirkabir Journal of Science and Research in Mechanical Engineering* **47**: 61-70.

[12] Esmailzadeh M., 2008, Three-dimensional modeling of curved structures containing and/or submerged in fluid, *Finite Elements in Analysis and Design* **44**: 334-345.

[13] Li H.-C., 2020, Free vibration of variable thickness FGM beam submerged in fluid, *Composite Structures* **233**: 111582.

[14] Malekzadeh K., Khalili S.M.R., Veysi Gorgabad A., 2015, Dynamic response of composite sandwich beams with arbitrary functionally graded cores subjected to low-velocity impact, *Mechanics of Advanced Materials and Structures* **22**: 605-618.

[15] Reddy J.N., 2003, *Mechanics of Laminated Composite Plates and Shells: Theory and Analysis*, CRC press.

[16] Reddy J.N., 2017, *Energy Principles and Variational Methods in Applied Mechanics*, John Wiley & Sons.

[17] Mindlin R.D., 1951, Influence of transverse shear deformation on the bending of classical plates, *Journal of Applied Mechanics, Transactions ASME* **8**: 18-31.

[18] Jeong K.-H., Amabili M., 2006, Bending vibration of perforated beams in contact with a liquid, *Journal of Sound and Vibration* **298**: 404-419.

[19] Yang M.,Qiao P., 2005, Higher-order impact modeling of sandwich structures with flexible core, *International Journal of Solids and Structures* **42**: 5460-5490.

[20] Frostig Y., Baruch M., 1994, Free vibrations of sandwich beams with a transversely flexible core: a high order approach, *Journal of Sound and Vibration* **176**: 195-208.

[21] Rahmani O., 2009, Free vibration analysis of sandwich structures with a flexible functionally graded syntactic core, *Composite Structures* **91**: 229-235.

[22] Malekzadeh F.K., 2012, Buckling analysis of composite sandwich panel with symmetric FGM core, using improved high-order theory, *Aerospace Mechanics Journal* **8**: 55-70.

[23] Nayak A.K., Shenoi R.A., Moy S.S.J., 2002, Analysis of damped composite sandwich plates using plate bending elements with substitute shear strain fields based on Reddy's higher-order theory, *Proceedings of the Institution of Mechanical Engineers, Part C: Journal of Mechanical Engineering Science* **216**: 591-606.

[24] Rahmanei H., Jafari A.A., 2016, Vibration analysis of a rectangular composite plate in contact with fluid, *Iranian Journal of Mechanical Engineering Transactions of the ISME* **17**: 67-83.